



Cite this: *RSC Adv.*, 2019, 9, 25048

# Cell changes and differential proteomic analysis during biodegradation of decabromodiphenyl ether (BDE-209) by *Pseudomonas aeruginosa*

Yu Liu,<sup>abc</sup> Zhe Liu,<sup>ab</sup> Aijun Gong,<sup>id</sup>\*<sup>ab</sup> Lina Qiu,<sup>ab</sup> Weiwei Zhang,<sup>ab</sup> Jingrui Li,<sup>ab</sup> Fukai Li,<sup>ab</sup> Yuzhen Bai,<sup>ab</sup> Jiandi Li<sup>ab</sup> and Ge Gao<sup>ab</sup>

Decabromodiphenyl ether (BDE-209) is a brominated flame retardant widely used in the world which, being an emerging persistent organic pollutant, poses a great potential hazard to both human health and the ecological environment. Microbial biodegradation has been considered as an effective and environment-friendly technique to remediate BDE-209. *Pseudomonas aeruginosa*, a Gram-negative bacterium capable of degrading BDE-209, was isolated from PBDEs-contaminated soil. To promote microbial biodegradation of BDE-209 and gain further insight into its mechanism, cell changes and differential proteomic analysis of *P. aeruginosa* during biodegradation were studied. The results showed that high cell surface hydrophobicity of *P. aeruginosa* make the bacteria absorb BDE-209 more easily. The increase in cell membrane permeability was caused by the *P. aeruginosa* responding to BDE-209 stress. IR spectra showed that hydroxyl, amide and CH<sub>2</sub> groups in the *P. aeruginosa* cell surface were involved in the interactions between BDE-209 with *P. aeruginosa*. The apoptotic-like cell changes and cell surface morphology changes were observed by flow cytometry (FCM) and field emission scanning electron microscopy (FESEM), respectively. Differentially expressed protein was analysed by two-dimensional electrophoresis (2-DE) and 40 protein spots were identified to be different after 5 days biodegradation.

Received 25th January 2019  
 Accepted 5th August 2019

DOI: 10.1039/c9ra00664h

[rsc.li/rsc-advances](http://rsc.li/rsc-advances)

## 1 Introduction

Polybrominated diphenyl ethers (PBDEs), a class of brominated flame retardants (BFRs), are widely used as flame retardants in a variety of consumer products, such as plastics, textiles, electronic goods and construction materials.<sup>1</sup> There are three major commercial formulations of PBDEs, which differ in the degree of bromination: penta-BDE, octa-BDE and deca-BDE.<sup>2</sup> Penta-BDE and octa-BDE were banned under the Stockholm Convention in 2009. Deca-BDE (mainly BDE-209) was phased out in Europe and completely banned in the US in 2013. However, it is still produced and used in large quantities in some parts of the world.<sup>3,4</sup> Due to the widespread use, chemical persistence and bioaccumulation, BDE-209 has been detected as the predominant BDE congener in atmosphere, water, soil, sediment, dust, especially in biota and humans, and its level has been increasing

since 1970s.<sup>5</sup> Many toxicological studies have demonstrated that exposure to BDE-209 can lead to neurobehavioral toxicity, thyroid hormone disruption, cancer and reproductive toxicity.<sup>6</sup> Therefore ongoing human exposure to BDE-209 may cause a potential risk to human health, and there is an urgent need to develop efficient methods for degrading and eliminating BDE-209.

Photolytic degradation, zerovalent iron (ZVI) degradation, and biodegradation are currently the major BDE-209 degradation methods.<sup>7</sup> Biodegradation have gained much attention due to its being environment-friendly and low-cost. Recent studies on biodegradation of BDE-209 using microbes mostly focus on detecting degradation characteristics and proposing degradation pathways,<sup>8,9</sup> but cell changes and differential proteomic analysis during biodegradation of BDE-209 are still unclear and deserve further investigation. *Pseudomonas aeruginosa* (*P. aeruginosa*), well capable of degrading BDE-209, could be used in bioremediation of the increasingly serious BDE-209-contamination. In the previous studies, Shi *et al.* reported the effect of cadmium ion on cell surface hydrophobicity (CSH) and membrane permeability variation during BDE-209 biodegradation by *Pseudomonas aeruginosa*. Results showed that direct adherence to the cell surface is the first step in biodegradation process,<sup>10</sup> but no other changes of cell surface have been reported so far. Moreover, we have reported the biodegradation of BDE-209 by crude enzyme extracted

<sup>a</sup>School of Chemistry and Biological Engineering, University of Science and Technology Beijing, Beijing 100083, China. E-mail: gongaijun5661@ustb.edu.cn; Fax: +86-10-82375661; Tel: +86-10-82375661

<sup>b</sup>Beijing Key Laboratory for Science and Application of Functional Molecular and Crystalline Materials, University of Science and Technology Beijing, Beijing 100083, China

<sup>c</sup>Institute of Biotechnology, Daqing Branch of Heilongjiang Academy of Science, Daqing 163319, China



from *P. aeruginosa*. Our results suggested that enzyme actually play the key role in the biodegradation process,<sup>11</sup> but it is unknown which kind of enzyme is responsible for the BDE-209 degradation. Up to now, differentially expressed protein in *P. aeruginosa* cell during biodegradation of BDE-209 have never been reported.

In this work, to better understand the mechanism of BDE-209 biodegradation in cell level, *P. aeruginosa* cell changes were examined by focusing on cell activity, cell surface hydrophobicity, cell membrane permeability, cell surface functional group and morphology. Moreover, differentially expressed protein during the biodegradation of BDE-209 by *P. aeruginosa* was also investigated.

## 2 Materials and experiments

### 2.1 Chemicals

Decabromodiphenyl ether (BDE-209, >99% purity) was purchased from Alfa Aesar (Tianjin, China). The single standard of BDE-209 was purchased from Sigma (St. Louis, USA). All other reagents were analytical grade and purchased from Sinopharm Chemical Reagent Beijing Co., Ltd (Beijing, China).

### 2.2 Bacterial strain cultivation

*Pseudomonas aeruginosa* (*P. aeruginosa*) was previously isolated from PBDEs-contaminated soil in China, and preserved by our laboratory. *P. aeruginosa* was enriched in 50 mL of beef extract peptone medium on a rotary shaker at 200 rpm and 30 °C for 30 h, followed by centrifugation at 8000g for 10 min at 4 °C. The harvested live cells were washed, resuspended, and cultivated in the mineral salt medium (MSM) with 20 mg L<sup>-1</sup> BDE-209 on a rotary shaker at 200 rpm and 35 °C.

The compositions of the beef extract peptone medium and the MSM medium were same as described in our previous research.<sup>11</sup>

### 2.3 BDE-209 biodegradation experiments

All BDE-209 biodegradation experiments were conducted in batch with 500 mL Erlenmeyer flasks. In each case, 6.0 mg BDE-209 and 300 mL MSM were added into a flask and mixed ultrasonically for 15 min to get a suspension. Afterwards, 120 mg live *P. aeruginosa* was transferred to the suspension and cultured on a rotary shaker at 200 rpm and 35 °C for 7 days. It was appropriate to keep cell density around 1 × 10<sup>8</sup> cells per mL. As for the control, dead *P. aeruginosa* instead of live cells was used. At the degradation time of 0, 1, 3, 5, 7 days, the quantification of BDE-209 was determined by using a gas chromatograph-mass spectrometer (GC-MS). BDE-209 degradation efficiency was calculated using the following equation:

$$\text{Degradation efficiency (\%)} = (1 - C_1/C_0) \times 100,$$

where  $C_0$  and  $C_1$  were the initial and residual BDE-209 concentration, respectively.

### 2.4 Flow cytometry (FCM) analysis

*P. aeruginosa* cells cultivated in MSM containing 20 mg L<sup>-1</sup> BDE-209 at different biodegradation time were harvested by centrifugation and washed twice with PBS buffer (pH 7.0), then re-suspended in 200 μL binding buffer with 5 μL Annexin V-FITC and 10 μL PI. The mixture was incubated in the dark at room temperature for 20 min to allow for complete staining. Live, apoptotic, and dead cell populations were analyzed by flow cytometry (BD FACSCalibur), and data were analyzed using FlowJo software (v10.0.7). The control was conducted under same condition but in the absence of BDE-209.

### 2.5 Cell surface characteristics analysis

**2.5.1 Cell surface hydrophobicity (CSH).** Cell surface hydrophobicity (CSH) was determined using the modified method of microbial adhesion to hydrocarbons (MATH).<sup>12</sup> *P. aeruginosa* cells cultivated in MSM containing 20 mg L<sup>-1</sup> BDE-209 at different degradation time were harvested, washed twice and re-suspended in PBS buffer (pH 7.0) to give an optical density of 0.5 at 600 nm ( $A_0$ ). 1 mL of xylene was added to 3 mL of cell suspension, vortexed for 2 min and incubated for an additional 20 min at room temperature. Finally, the aqueous phase was removed and its optical density at 600 nm ( $A_1$ ) was measured. CSH was calculated using the formula:  $\text{CSH (\%)} = (1 - A_1/A_0) \times 100$ . The control was conducted under same condition but in the absence of BDE-209.

**2.5.2 Cell membrane permeability.** Cell membrane permeability of *P. aeruginosa* was evaluated by measuring the release of β-galactosidase activity into the culture medium using *o*-nitrophenyl-β-D-galactopyranoside (ONPG) as a substrate.<sup>13</sup> Pre-cultivated bacteria was pipetted into Erlenmeyer flasks containing 100 mL MSM and 1% lactose, and incubated on a rotary shaker at 35 °C for 10 h. Then the solutions were centrifuged at 8000g for 5 min, washed three times and re-suspended in β-galactosidase buffer. To the buffer was added BDE-209 at 20 mg L<sup>-1</sup> then mixed with ONPG at 1 mg mL<sup>-1</sup>. The control was conducted in the solution without BDE-209. Cell membrane permeability was measured by UV-spectrophotometer at 405 nm.

**2.5.3 Fourier transform infrared spectroscopy (FTIR).** FTIR was used to characterize the cell surface functional groups of *P. aeruginosa*. *P. aeruginosa* cells cultivated in MSM containing 20 mg L<sup>-1</sup> BDE-209 at different degradation time were harvested, washed twice with MSM and dried in a freeze drier at -50 °C for 30 h. Samples were scanned in the 4000–400 cm<sup>-1</sup> region using a FTIR spectrometer (Nicolet iS10, Thermo Fisher, USA). The control was conducted under same condition but in the absence of BDE-209.

**2.5.4 Field emission scanning electron microscopy (FESEM).** Surface morphology of *P. aeruginosa* was observed under a FESEM (SU8010, Hitachi, Japan). *P. aeruginosa* cells cultivated in MSM containing 20 mg L<sup>-1</sup> BDE-209 at different degradation time were harvested and subjected to a series of pre-treatment processes including washing with



PBS, fixation with glutaraldehyde, gradient dehydration with water-ethanol solutions, replacement with tertiary butyl alcohol and freeze drying. Finally, the dried samples were mounted on a conducting resin and sputter-coated with gold prior to the FESEM analysis. The control was conducted under same condition but in the absence of BDE-209.

## 2.6 Differentially expressed protein analysis

*P. aeruginosa* cultured for 5 days in MSM with or without BDE-209 ( $20 \text{ mg L}^{-1}$ ) were harvested by centrifugation at  $6000g$  and  $4^\circ\text{C}$  for 15 min and washed three times with cold PBS. The cell pellet was resuspended in the lysis buffer, and then cells were disrupted by sonication in an ice bath. The protein extracts underwent ultracentrifugation for 45 min at  $12\,000g$  and  $4^\circ\text{C}$ . Afterwards, the obtained supernatants were purified using 2-D Clean-Up Kit (Amersham Biosciences, USA) and the protein concentration was determined by 2-D Quant Kit (Amersham Biosciences, USA) with bovine serum albumin as a standard. Two-dimensional electrophoresis (2-DE) was performed based on the method described by Liu *et al.*<sup>14</sup> For the first dimension, isoelectric focusing (IEF),  $500 \mu\text{g}$  of protein was loaded onto an immobilized pH gradient (IPG) strip (24 cm, pH 4–7). After IEF separation, the IPG strips were equilibrated in two equilibration buffer for 15 min as described by Song *et al.*<sup>15</sup> Then the proteins were further separated on 12.5% SDS-polyacrylamide gels for the second dimension. After the completion of 2-DE, gels were stained with Coomassie brilliant blue, scanned using Image-Scanner III (GE Healthcare) and analyzed with ImageMaster 2D Platinum software (Version 7.0, GE Healthcare). Altered abundances of spots were standardized and then compared based on their volume percentages in the total spot volume over the whole gel image. Significantly changed spots were selected by the rate increased/decreased  $\geq 2$ -fold or complete appearance and disappearance. Differentially expressed proteins were excised from the gels and digested with trypsin and analyzed by a 4800 Plus MALDI TOF/TOF mass spectrometer (Applied Biosystems, Foster City, USA). Both the MS and MS/MS data were integrated and processed using the GPS Explorer V3.6 software (Applied Biosystems, USA) and searched against the NCBI database using Mascot V2.1 software (Matrix Science, UK). Protein scores greater than 65 were significant and accepted.

## 2.7 Extraction and analytical methods

For the extraction procedure, we refer to previous work.<sup>11</sup> The analytical method for BDE-209 was the same as in the literature<sup>16</sup> and analysis by 7890-5975c GC-MS (Agilent, USA) equipped with a DB-5 MS column ( $60 \text{ m} \times 0.25 \text{ mm} \times 0.25 \mu\text{m}$ ). The quantification was performed with a five-point standard curve of BDE-209.

## 2.8 Quality assurance and quality control

All experiments were performed in triplicate and the mean values were given. The standard deviations ranged from 1.0% to 5.0%.

# 3 Results

## 3.1 BDE-209 biodegradation by *P. aeruginosa*

Fig. 1 shows the degradation efficiency of BDE-209 by *P. aeruginosa* during biodegradation time. As shown, the degradation efficiency of BDE-209 rose slowly in day 1 and then ascended sharply from day 3, finally levelled off after 5 days. This trend was in accordance with Shi's work,<sup>10</sup> but changes in cellular properties during the biodegradation of BDE-209 by *P. aeruginosa* were not discussed deeply. Hence, in the following, we focused on cell changes of *P. aeruginosa* during degradation time.

## 3.2 Apoptotic-like cell changes of *P. aeruginosa* during BDE-209 biodegradation

To quantitatively gain insight into apoptotic-like cell changes of *P. aeruginosa* during BDE-209 biodegradation, a display of PI versus Annexin V-FITC fluorescence was measured by FCM analysis (Fig. 2). As shown in Fig. 2, four groups of cells were clearly seen in each acquired data plot: dead cells (Q1, positive for PI and negative for Annexin V-FITC), late apoptotic cells (Q2, positive for PI and Annexin V-FITC), live cells (Q3, negative for PI and Annexin V-FITC), early apoptotic cells (Q4, negative for PI and positive for Annexin V-FITC). From the results it can be observed, *P. aeruginosa* cells treated with  $20 \text{ mg L}^{-1}$  BDE-209 in day 1 and day 7 exhibited an increase of apoptosis and death compared to day 0. The total apoptosis rate first increased to 1.17% in the day 1 as compared to that in day 0 (0.22%), then declined in day 3 and day 5, finally increased to 2.63% in day 7. Moreover, cells treated with BDE-209 showed the highest population of dead cells (5.84%) in day 1. For *P. aeruginosa* cells in control, cell death increased in day 1 (3.23%) and day 3 (4.11%), then cell apoptosis began to increase from day 5 (0.46%), and reached 1.97% in day 7.

## 3.3 Cell surface changes during BDE-209 biodegradation

### 3.3.1 Changes in CSH and cell membrane permeability.

Fig. 3 shows the changes of CSH and cell membrane

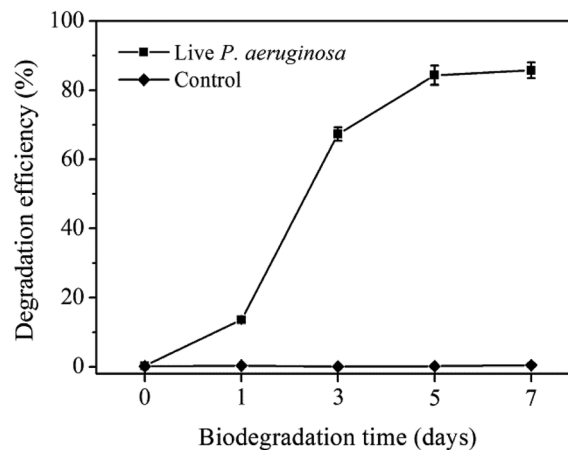


Fig. 1 Degradation efficiency of  $20 \text{ mg L}^{-1}$  BDE-209 under incubation time.



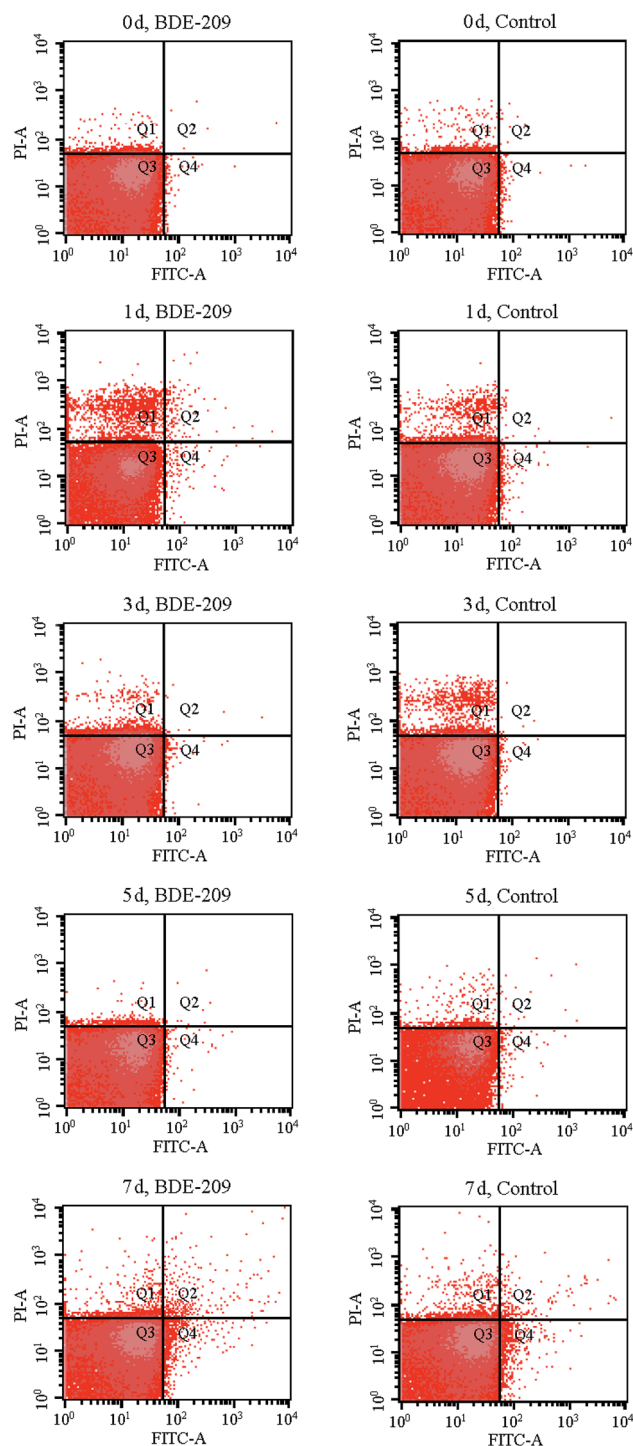


Fig. 2 Apoptotic-like cell changes of *P. aeruginosa* after treatment with  $20 \text{ mg L}^{-1}$  BDE-209 and without BDE-209 (control) for 0–7 days. Four quadrants (Q) are representing: (Q1) dead cells; (Q2) late apoptotic cells; (Q3) live cells; (Q4) early apoptotic cells.

permeability of *P. aeruginosa* treated with and without BDE-209. In the presence of BDE-209, the CSH first maintained at high level from 48.3% to 52.1% until day 3 and then decreased markedly from the 5th day. The cell membrane permeability increased gradually from day 1 to 3 then sharply from day 5 to 7.

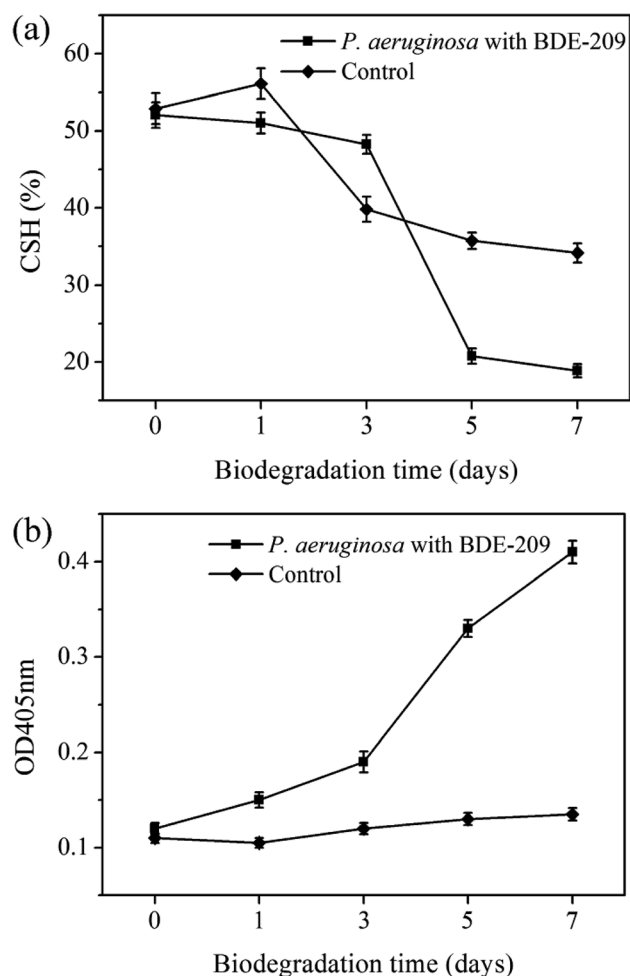


Fig. 3 Changes of CSH (a) and cell membrane permeability (b) of *P. aeruginosa* during BDE-209 biodegradation.

In the absence of BDE-209, both CSH and cell membrane permeability changes less obviously.

**3.3.2 FTIR analysis.** The functional groups present on the cell surface of *P. aeruginosa* during BDE-209 biodegradation were explored to reveal the cell surface changes through FTIR analysis as shown in Fig. 4. The peak assignments of *P. aeruginosa* were as follows:  $1086 \text{ cm}^{-1}$  and  $1236 \text{ cm}^{-1}$  were ascribed to P=O stretching vibration of phosphate groups,  $1398 \text{ cm}^{-1}$  ascribed to C–O stretching vibration of –COOH,  $1455 \text{ cm}^{-1}$  ascribed to C–H bending vibration of –CH<sub>2</sub>,  $1544 \text{ cm}^{-1}$  ascribed to N–H and C–N in amide groups,  $1651 \text{ cm}^{-1}$  and  $1741 \text{ cm}^{-1}$  ascribed to C=O stretching vibration,  $2925 \text{ cm}^{-1}$  and  $2958 \text{ cm}^{-1}$  ascribed to C–H stretching vibration,  $3296 \text{ cm}^{-1}$  ascribed to O–H stretching vibration.<sup>17</sup> For *P. aeruginosa* cells treated with BDE-209, the peaks at  $3296$ ,  $1651$  and  $1544 \text{ cm}^{-1}$  become broader, and the intensity of peaks  $2925 \text{ cm}^{-1}$  decreased gradually. In control, less obvious changes with time were observed.

**3.3.3 Changes in cell surface morphology.** Fig. 5 revealed the changes of cell surface morphology in presence and absence of BDE-209. In the presence of BDE-209, *P.*



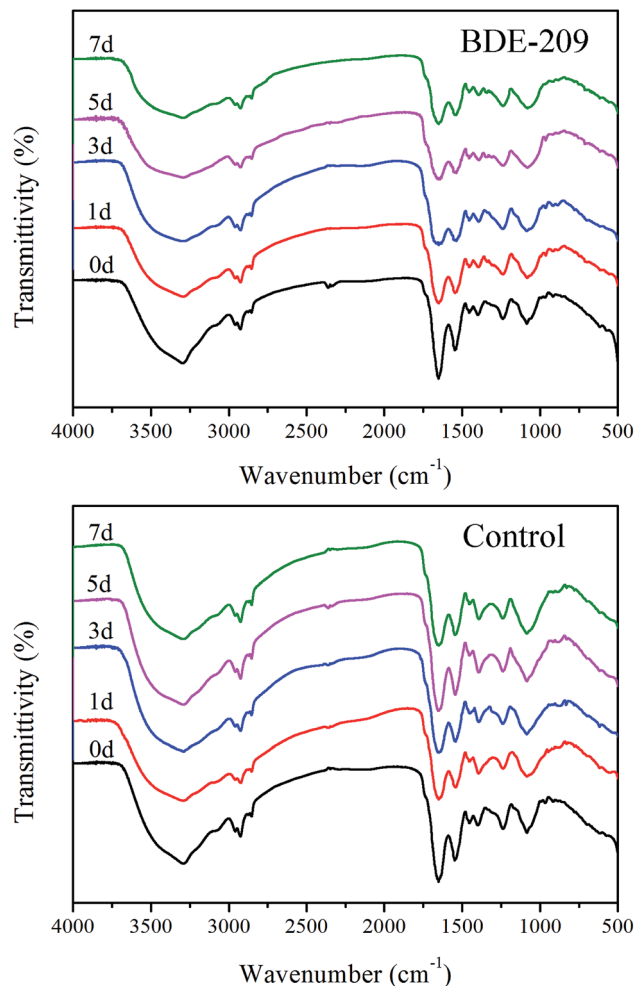


Fig. 4 FTIR spectrum of the *P. aeruginosa* cells treated with  $20 \text{ mg L}^{-1}$  BDE-209 and without BDE-209 (control) at the degradation time of 0–7 days.

*aeruginosa* cells were smooth and short rod-shaped just before BDE-209 degradation, but some cells tended to be plicated and irregular shaped at the BDE-209 degradation time of 1 day. While most cells became slender, smooth and short rod-shaped in day 3 and day 5. Finally, at the degradation time of 7 days, some cells were rough and atrophic in irregular shapes. In control, some cells tended to be slender in day 1, then changed to be rough and atrophic in irregular shapes from day 3.

### 3.4 Differentially expressed protein during BDE-209 biodegradation

To investigate protein changes in *P. aeruginosa* cells during BDE-209 biodegradation, a comparative proteomic approach was utilized to identify differentially expressed proteins from *P. aeruginosa* cultured in MSM without BDE-209 and with  $20 \text{ mg L}^{-1}$  BDE-209. Representative maps of the proteins separated on a 2-DE gel were shown in Fig. 6. Approximately 40 protein spots were identified to be different after 5 days

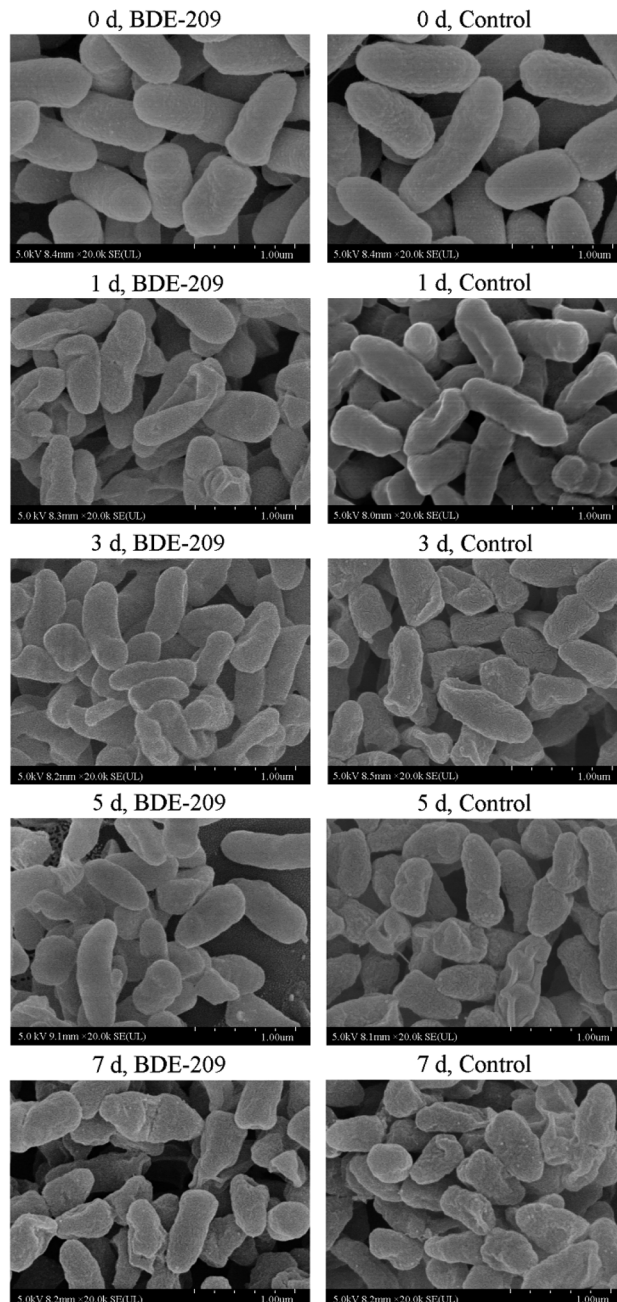


Fig. 5 FESEM images of the *P. aeruginosa* cells treated with  $20 \text{ mg L}^{-1}$  BDE-209 and without BDE-209 (control) at the degradation time of 0–7 days.

biodegradation. Out of them, seven protein spots in the same location of Fig. 6a and b exhibited significant changes at the level of protein expression, they were named as 1–7. Spots 8–11, and spots 12–40 were those spots that only appeared in Fig. 6a and b, respectively. The 40 spots were analysed by MALDI-TOF-TOF with a significant mascot score  $> 65$  ( $p$ -value  $< 0.05$ ), among which 12 identified spots are shown in Table 1. Table 1 summarizes details of these identified proteins including their protein names, accession numbers and other MS data.



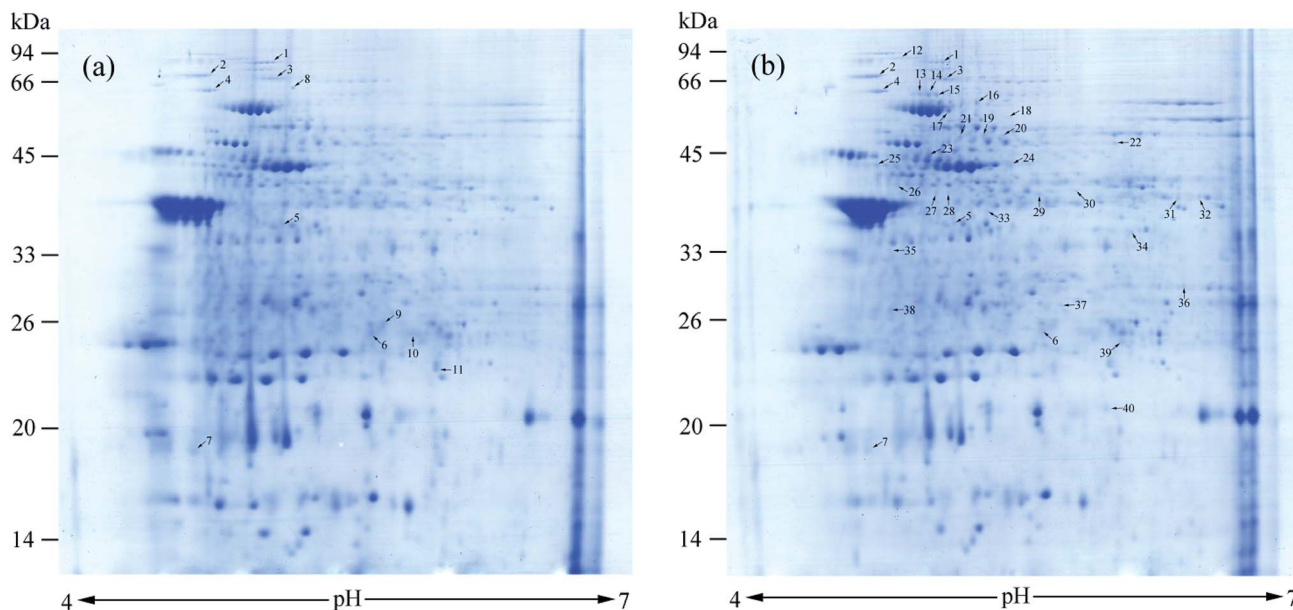


Fig. 6 Representative 2-DE gels of proteome from *P. aeruginosa* cultured in MSM without BDE-209 (a) and with 20 mg L<sup>-1</sup> BDE-209 (b). The 40 differentially expressed proteins during BDE-209 biodegradation are marked by numbers on the gels, and were analyzed by MALDI-TOF/TOF mass spectrometry.

Table 1 List of protein spots which were differentially expressed in *P. aeruginosa* with 20 mg L<sup>-1</sup> BDE-209 for 5 days

Spots no	Protein name	Accession number	MW	PI	Mascot score	Peptides matched	Coverage (%)
1	Peroxiredoxin	gi 1279400824	20 643	5.89	760	93	65
2	Molecular chaperone GroEL	gi 1279402470	57 107	5.04	536	47	9
3	30S ribosomal protein S1	gi 1279398492	61 946	4.83	2432	203	45
12	Outer membrane protein assembly factor BamA	gi 1279401791	88 150	5.06	151	12	8
16	NAD-dependent succinate-semialdehyde dehydrogenase	gi 1279399219	51 875	5.60	7433	400	62
18	Isocitrate dehydrogenase (NADP(+))	gi 518511667	45 689	5.10	1629	11	28
23	2-Phosphoglycerate dehydratase	gi 13124125	45 338	5.04	3059	202	68
24	Agmatine deiminase	gi 1279399248	41 564	4.84	761	39	20
32	L-Asparaginase	gi 1279400388	38 620	6.67	3026	249	52
35	Electron transfer flavoprotein subunit beta	gi 518513080	26 535	4.85	1912	164	64
38	ATP synthase subunit alpha	gi 1279400601	55 530	5.33	845	67	29
40	dTDP-4-dehydrorhamnose 3,5-epimerase	gi 81622016	20 924	5.74	542	76	61

## 4 Discussion

In the biodegradation process of harmful and toxic organic contaminants, microbes resist organic contaminants at the beginning, and then the interaction between microbes and contaminants leads to a series of cellular characteristic changes.<sup>18</sup> In this work, we have found that *P. aeruginosa* had a series of cellular characteristic changes during the biodegradation of BDE-209. When BDE-209 biodegradation had just began (day 0), *P. aeruginosa* treated with and without BDE-209 both grew well and had normal cell morphology. In day 1, BDE-209 degradation efficiency was low. Compared with control, *P. aeruginosa* treated with BDE-209 caused a larger population of apoptotic and dead cells, accompanied by the

appearance of plicated and irregular shaped cells. Apoptosis is a form of programmed cell death (PCD) that is essential in eliminating old, unnecessary or damaged cells to maintain appropriate cell numbers and protect bacteria against poor environment.<sup>19,20</sup> So this is probably because the initial exposure of *P. aeruginosa* to BDE-209 lead to resistance, some cells become deformed, and then apoptosis appears to protect bacteria against BDE-209 stress.<sup>21</sup> In day 3 and 5, BDE-209 degradation efficiency increased apparently, apoptotic and dead cell decreased, cell morphology return to normal. This is probably because *P. aeruginosa* has adapted to BDE-209 gradually, followed by degrading BDE-209 as carbon source for metabolism.<sup>22</sup> As for control, these changes were not observed. In day 7, no matter *P. aeruginosa* was treated with or without



BDE-209, cell apoptosis and death appeared, and cells became rough and atrophic. This is probably because the quantity of nutrients in the culture medium declined and growing environment became unfavorable.<sup>23</sup>

One of most common mechanisms explains that hydrophobic BDE-209 first adheres to the hydrophobic regions of the cell surface, then enters the cell through cell membrane, finally is degraded by intracellular enzymes.<sup>24,25</sup> For this reason, CSH and cell membrane permeability are the most important factors in determining whether BDE-209 can be successfully adsorbed onto the surface of cells and enter into the cells. In this experiment, we have found that CSH maintained at a high level till day 3, making *P. aeruginosa* adsorb hydrophobic BDE-209 more easily. Then CSH decreased markedly from day 5. Meanwhile, the cell membrane permeability increased gradually from day 1 then sharply from day 5. The increase in cell membrane permeability was caused by the *P. aeruginosa* responding to BDE-209 stress. The membrane structure was changed due to the sharply increased cell membrane permeability and the hydrophobic regions was disrupted, which may be part of the reason for the decline of CSH of *P. aeruginosa*.<sup>20</sup>

*P. aeruginosa* is a Gram-negative bacterium. Its cell wall is mainly composed of polysaccharides, phospholipids and proteins, characteristic of carboxyl, phosphate, and amino groups, which can be assigned to in IR spectra (Fig. 4).<sup>26</sup> During degradation, the changed peaks suggested that hydroxyl, amide and CH<sub>2</sub> groups were involved in the interactions between BDE-209 and *P. aeruginosa*. In control, these peaks did not change obviously with time. All the above results indicated that polysaccharides and proteins in the cell walls of *P. aeruginosa* may play critical roles in the binding of BDE-209.<sup>27</sup>

2-DE is an effective tool for gaining insight into physiological changes at cellular level.<sup>28</sup> Thus analysis and identification of differentially expressed proteins during BDE-209 biodegradation could give us an insight into cell changes in this process. In this experiment, 12 differentially expressed proteins were identified and listed in Table 1. Peroxidase can degrade BDE-209, Li *et al.* found that manganese peroxidase plays an important role in BDE-209 depletion.<sup>29</sup> 30S ribosomal protein S1, which can bind to a specific site of mRNA, starts protein synthesis.<sup>30</sup> Electron transfer flavoprotein can transfer the electrons to the main respiratory chain.<sup>31</sup> Outer membrane protein can form a stable folding intermediate, which keeps the Gram-negative bacterium survive under stress conditions.<sup>32</sup> Molecular chaperone works to prevent outer membrane protein being adsorbed to outer membrane by capturing and stabilizing its folding intermediates.<sup>33</sup> Therefore, these enzymes help *P. aeruginosa* adapt to restricted BDE-209 conditions, reduce toxicity, and maintain the normal metabolism of cells.<sup>34</sup> NAD-dependent succinate-semialdehyde dehydrogenase, isocitrate dehydrogenase and 2-phosphoglycerate dehydratase were probably attributed to the resistance systems of *P. aeruginosa* to the oxidative stress induced by BDE-209.<sup>35</sup> ATP synthase generates energy in the form of ATP, which was confirmed to play an important role in BDE biodegradation.<sup>36</sup> The roles of agmatine deiminase, L-asparaginase and dTDP-4-dehydrorhamnose 3,5-epimerase in BDE-209 degradation is not known yet and further study is still needed.

## 5 Conclusions

Collectively, both cell surface and intracellular enzyme changes in the biodegradation of BDE-209 by *P. aeruginosa*. The apoptotic-like cell changes and cell surface morphology changes were observed during the biodegradation of BDE-209 by *P. aeruginosa*. The results showed that high CSH of *P. aeruginosa* facilitated the attachment of BDE-209 to cell surface. The increase in cell membrane permeability caused by *P. aeruginosa* responding to BDE-209 stress favored BDE-209 penetrating into cells and being degraded. IR spectra showed that polysaccharides and proteins in the cell walls of *P. aeruginosa* may participate in binding BDE-209. Differentially expressed protein was analysed through 2-DE, among which peroxidase and ATP synthase play a critical role in BDE-209 degradation. As far as we know, this is the first report on investigating cell changes and differentially expressed proteins during biodegradation of BDE-209 by *P. aeruginosa*. These explorations offer new insights into the mechanism of BDE-209 biodegradation by *P. aeruginosa*.

## Conflicts of interest

There are no conflicts to declare.

## Acknowledgements

This work was financially supported by National Key R&D Program of China (No. 2017YFF0106006) and Chinese National Natural Science Foundation (No. 51701016).

## References

- 1 C. A. de Wit, *Chemosphere*, 2002, **46**, 583–624.
- 2 R. Quiroz, L. Arellano, J. O. Grimalt and P. Fernandez, *J. Chromatogr., A*, 2008, **1192**, 147–151.
- 3 A. Francois, R. Techer, M. Houde, P. Spear and J. Verreault, *Environ. Toxicol. Chem.*, 2016, **35**, 2215–2222.
- 4 H. W. Zhu, Y. Wang, X. W. Wang, T. G. Luan and N. F. Tam, *Sci. Total Environ.*, 2014, **468–469**, 130–139.
- 5 H. Stiborova, J. Vrkoslavova, P. Lovecka, J. Pulkrabova, P. Hradkova, J. Hajslova and K. Demnerova, *Chemosphere*, 2015, **118**, 315–321.
- 6 M. Li, Z. Liu, L. Gu, R. Yin, H. Li, X. Zhang, T. Cao and C. Jiang, *Front. Genet.*, 2014, **5**, 1–6.
- 7 B. Z. Wu, Y. J. Sun, Y. H. Chen, H. K. Yak, J. J. Yu, W. S. Liao, K. H. Chiu and S. M. Peng, *Chemosphere*, 2016, **157**, 115–123.
- 8 M. Lu, Z. Z. Zhang, X. J. Wu, Y. X. Xu, X. L. Su, M. Zhang and J. X. Wang, *Bioresour. Technol.*, 2013, **149**, 8–15.
- 9 G. Y. Xu and J. B. Wang, *Chemosphere*, 2014, **110**, 70–77.
- 10 G. Y. Shi, H. Yin, J. S. Ye, H. Peng, J. Li and C. L. Luo, *J. Hazard. Mater.*, 2013, **263**, 711–717.
- 11 Y. Liu, A. J. Gong, L. N. Qiu, J. R. Li and F. K. Li, *Int. J. Environ. Res. Public Health*, 2015, **12**, 11829–11847.
- 12 D. Y. Ren, C. Li, Y. Q. Qin, R. L. Yin, X. Li, M. Y. Tian, S. W. Du, H. H. Guo, C. X. Liu, N. Zhu, D. D. Sun, Y. Li and N. Y. Jin, *Anaerobe*, 2012, **18**, 508–515.



- 13 L. L. Wang, L. T. Tang, R. Wang, X. Y. Wang, J. S. Ye and Y. Long, *Environ. Sci. Pollut. Res.*, 2016, **23**, 5166–5178.
- 14 S. S. Liu, C. L. Guo, Z. Dang and X. J. Liang, *Ecotoxicol. Environ. Saf.*, 2017, **137**, 256–264.
- 15 Q. Q. Song, P. F. Zheng, L. G. Qiu, X. Jiang, H. W. Zhao, H. L. Zhou, Q. Han and X. P. Diao, *Toxicol. Lett.*, 2016, **240**, 185–195.
- 16 Y. Liu, A. J. Gong, L. N. Qiu, J. R. Li and F. K. Li, *MicrobiologyOpen*, 2017, **6**, 1–10.
- 17 N. Bai, S. Wang, R. Abuduaini, M. N. Zhang, X. F. Zhu and Y. H. Zhao, *Sci. Total Environ.*, 2017, **590–591**, 343–351.
- 18 S. S. Liu, C. L. Guo, X. J. Liang, F. J. Wu and Z. Dang, *Ecotoxicol. Environ. Saf.*, 2016, **129**, 210–218.
- 19 N. Allocati, M. Masulli, C. Di Ilio and V. De Laurenzi, *Cell Death Dis.*, 2015, **6**, e1609.
- 20 S. Tang, H. Yin, S. Chen, H. Peng, J. Chang, Z. Liu and Z. Dang, *J. Hazard. Mater.*, 2016, **308**, 335–342.
- 21 M. C. Ferrante, G. M. Raso, E. Esposito, G. Bianco, A. Iacono, M. T. Clausi, P. Amero, A. Santoro, R. Simeoli, G. Autore and R. Meli, *Toxicol. Lett.*, 2011, **202**, 61–68.
- 22 L. L. Liu, Y. C. Zhang, R. H. Liu, Z. P. Wang, F. Xu, Y. L. Chen and K. F. Lin, *Environ. Sci. Pollut. Res.*, 2016, **23**, 3925–3933.
- 23 H. Lee and D. G. Lee, *J. Microbiol. Biotechnol.*, 2019, **29**, 1014–1021.
- 24 L. Shapiro, *Cell*, 1993, **73**, 841–855.
- 25 Z. Wu, M. Xie, Y. Li, G. Gao, M. Bartlam and Y. Wang, *Amb. Express*, 2018, **8**, 27.
- 26 S. Luo, L. L. Li, A. W. Chen, Q. R. Zeng, H. Xia and J. D. Gu, *Chemosphere*, 2017, **178**, 187–196.
- 27 N. Bai, S. Wang, R. Abuduaini, M. Zhang, X. F. Zhu and Y. H. Zhao, *Sci. Total Environ.*, 2017, **590**, 343–351.
- 28 Z. W. Cheng, Z. Y. Chen, X. Yan, Y. W. Bian, X. Deng and Y. M. Yan, *J. Proteomics*, 2018, **170**, 1–13.
- 29 X. Li, A. Y. Chen, Y. Wu, L. Wu, L. Xiang, H. M. Zhao, Q. Y. Cai, Y. W. Li, C. H. Mo, M. H. Wong and H. Li, *Sci. Total Environ.*, 2018, **634**, 417–426.
- 30 M. P. Kalapos, H. Paulus and N. Sarkar, *Biochimie*, 1997, **79**, 493–502.
- 31 C. L. Hall and J. D. Lambeth, *J. Biol. Chem.*, 1980, **255**, 3591–3595.
- 32 K. Chourabi, F. Torrella, S. Kloula, J. A. Rodriguez, I. Trabelsi, S. Campoy, A. Landoulsi and A. Chatti, *Arabian J. Geosci.*, 2017, **10**, 1–7.
- 33 R. N. Reusch, *FEBS J.*, 2012, **279**, 894–909.
- 34 J. Xu, H. Q. Wang and D. K. Kong, *IOP Conf. Ser. Earth Environ. Sci.*, 2018, **111**, 012032.
- 35 A. K. Felux, D. Spiteller, J. Klebensberger and D. Schleheck, *Proc. Natl. Acad. Sci.*, 2015, **112**, E4298–E4305.
- 36 M. Feng, H. Yin, H. Peng, X. T. Liu, P. P. Yang, G. N. Lu and Z. Dang, *Ecotoxicol. Environ. Saf.*, 2017, **142**, 388–398.

